

AD-A140 033

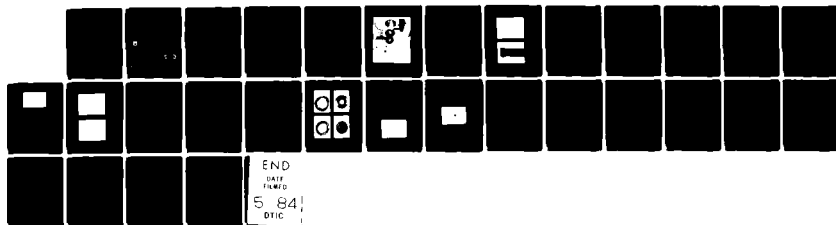
A Z-PINCH PHOTO-PUMPED PULSED ATOMIC IODINE LASER(U)
AIR FORCE WEAPONS LAB KIRTLAND AFB NM D H STONE ET AL.
MAR 84 AFWL-TR-83-33

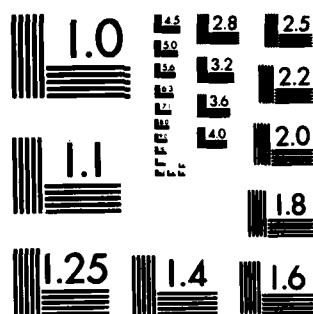
1/-

UNCLASSIFIED

F/G 20/5

NL





MICROCOPY RESOLUTION TEST CHART
NATIONAL BUREAU OF STANDARDS-1963-A

(2)

AD A140033

A Z-PINCH PHOTO-PUMPED PULSED ATOMIC IODINE LASER

David H. Stone
David P. Saunders
Miles C. Clark

March 1984



Final Report

Approved for public release; distribution unlimited.

DTIC
ELECTE
APR 12 1984
S B D

DTIC FILE COPY

AIR FORCE WEAPONS LABORATORY
Air Force Systems Command
Kirtland Air Force Base, NM 87117

84 04 11 049

This final report was prepared by the Air Force Weapons Laboratory, Kirtland Air Force Base, New Mexico, under Job Order ILIR8217. Captain David H. Stone (NTYP) was the Laboratory Project Officer-in-Charge.

When Government drawings, specifications, or other data are used for any purpose other than in connection with a definitely Government-related procurement, the United States Government incurs no responsibility or any obligation whatsoever. The fact that the Government may have formulated or in any way supplied the said drawings, specifications, or other data, is not to be regarded by implication, or otherwise in any manner construed, as licensing the holder, or any other person or corporation; or as conveying any rights or permission to manufacture, use, or sell any patented invention that may in any way be related thereto.

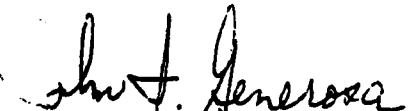
This report has been authored by an employee of the United States Government. Accordingly, the United States Government retains a nonexclusive, royalty-free license to publish or reproduce the material contained herein, or allow others to do so, for the United States Government purposes.

This report has been reviewed by the Public Affairs Office and is releasable to the National Technical Information Service (NTIS). At NTIS, it will be available to the general public, including foreign nationals.

If your address has changed, if you wish to be removed from our mailing list, or if your organization no longer employs the addressee, please notify AFWL/NTYP, Kirtland AFB, NM 87117 to help us maintain a current mailing list.

This report has been reviewed and is approved for publication.


MILES C. CLARK
Project Officer


JOHN I. GENEROSA
Lt Colonel, USAF
Chief, Advanced Laser Branch

FOR THE COMMANDER

ALAN R. COLE
Colonel, USAF
Chief, Advanced Laser Technology Div

DO NOT RETURN COPIES OF THIS REPORT UNLESS CONTRACTUAL OBLIGATIONS OR NOTICE ON A SPECIFIC DOCUMENT REQUIRES THAT IT BE RETURNED.

UNCLASSIFIED

AD-A140033

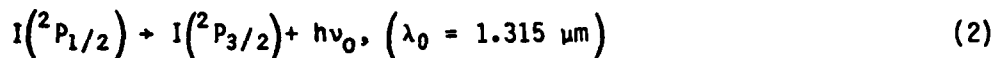
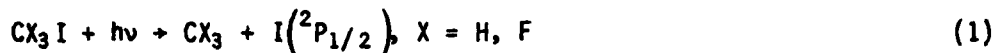
SECURITY CLASSIFICATION OF THIS PAGE

REPORT DOCUMENTATION PAGE

1a. REPORT SECURITY CLASSIFICATION UNCLASSIFIED		1b. RESTRICTIVE MARKINGS	
2a. SECURITY CLASSIFICATION AUTHORITY		3. DISTRIBUTION/AVAILABILITY OF REPORT Approved for public release; distribution unlimited.	
2b. DECLASSIFICATION/DOWNGRADING SCHEDULE			
4. PERFORMING ORGANIZATION REPORT NUMBER(S) AFWL-TR-83-33		5. MONITORING ORGANIZATION REPORT NUMBER(S) AFWL-TR-83-33	
6a. NAME OF PERFORMING ORGANIZATION Air Force Weapons Laboratory	6b. OFFICE SYMBOL (If applicable) NTYP	7a. NAME OF MONITORING ORGANIZATION Air Force Weapons Laboratory	
6c. ADDRESS (City, State and ZIP Code) Kirtland Air Force Base, NM 87117		7b. ADDRESS (City, State and ZIP Code) Kirtland Air Force Base, NM 87117	
8a. NAME OF FUNDING/SPONSORING ORGANIZATION Air Force Weapons Laboratory	8b. OFFICE SYMBOL (If applicable) NTYP	9. PROCUREMENT INSTRUMENT IDENTIFICATION NUMBER	
8c. ADDRESS (City, State and ZIP Code) Kirtland Air Force Base, NM 87117		10. SOURCE OF FUNDING NOS.	
		PROGRAM ELEMENT NO. 61101F	PROJECT NO. ILIR
		TASK NO. 82	WORK UNIT NO. 17
11. TITLE (Include Security Classification) A Z-PINCH PHOTO - PUMPED PULSED ATOMIC IODINE LASER			
12. PERSONAL AUTHOR(S) David H. Stone, David P. Saunders, Miles C. Clark			
13a. TYPE OF REPORT Final	13b. TIME COVERED FROM 10/81 TO 09/82	14. DATE OF REPORT (Yr., Mo., Day) 1984 March	15. PAGE COUNT 28
16. SUPPLEMENTARY NOTATION			
17. COSATI CODES		18. SUBJECT TERMS (Continue on reverse if necessary and identify by block number)	
FIELD 20	GROUP 05	Z-pinch	
		Pulsed Iodine	
		Power Compression	
		Coaxial Pump	
19. ABSTRACT (Continue on reverse if necessary and identify by block number)			
<p>A pulsed atomic iodine laser (CF_3I) was designed and constructed using a coaxial xenon flash lamp as a pump source. The flash lamp was operated at low pressure to obtain pulse compression via xenon self-pinch. Electrical and optical diagnostics were performed for various xenon and CF_3I pressures. Calorimeter data and burn patterns were obtained for the laser. Time-resolved spectroscopic data were taken throughout the CF_3I pump band.</p>			
20. DISTRIBUTION/AVAILABILITY OF ABSTRACT UNCLASSIFIED/UNLIMITED <input checked="" type="checkbox"/> SAME AS RPT. <input type="checkbox"/> DTIC USERS <input type="checkbox"/>		21. ABSTRACT SECURITY CLASSIFICATION UNCLASSIFIED	
22a. NAME OF RESPONSIBLE INDIVIDUAL David H. Stone	22b. TELEPHONE NUMBER (Include Area Code) 505-844-0121	22c. OFFICE SYMBOL AFWL (NTYP)	

I. INTRODUCTION

The photo-initiated atomic iodine laser was discovered in 1964, when Kasper and Pimentel (Ref. 1) observed stimulated emission at $\lambda = 1.315 \mu\text{m}$, following flash photolysis of either CF_3I or CH_3I . Lasing occurs via the following schemes:



Reference 2 describes iodine laser physics and applications and provides an extensive bibliography. More recent studies (e.g., Ref. 3) have focused on laser fusion applications requiring high beam quality and intense mode-locked or Q-switched pulses.

This report describes a pulsed CF_3I laser using a Z-pinch coaxial xenon flash lamp. Z-pinch flash lamps are well known, but have not been applied to the iodine laser. Figure 1 is a photograph of the iodine laser shown schematically in Figure 2. There are several advantages in operating the outer cylinder in the Z-pinch mode. Pulse compression is achieved as the electrical discharge energy is converted into the dynamic energy of the pinch. As the xenon is crushed in an annulus around the inner tube, ultraviolet (UV) radiation is extracted in a time short compared to the electrical time constant. Figure 3 shows two heavily filtered open-shutter photographs of the enhanced light output in the annulus immediately surrounding the inner tube. Another advantage of the pinch is that for a given capacitor bank voltage and energy, the current density is greatly increased, thus producing a greater flux of UV pump energy.

1. Kasper, J. V. and Pimentel, G. C., Applied Physics Letters 5, 231, 1964.
2. Hohla, K. and Kompa, K., "The Photochemical Iodine Laser," Handbook of Chemical Lasers, ed. R. Gross and J. Bott, John Wiley & Sons, 1976.
3. Palmer, R. E., Padrick, T. D. and Palmer, M. A., Opt. and Quantum Elec. 11, pp. 61-70, 1979.

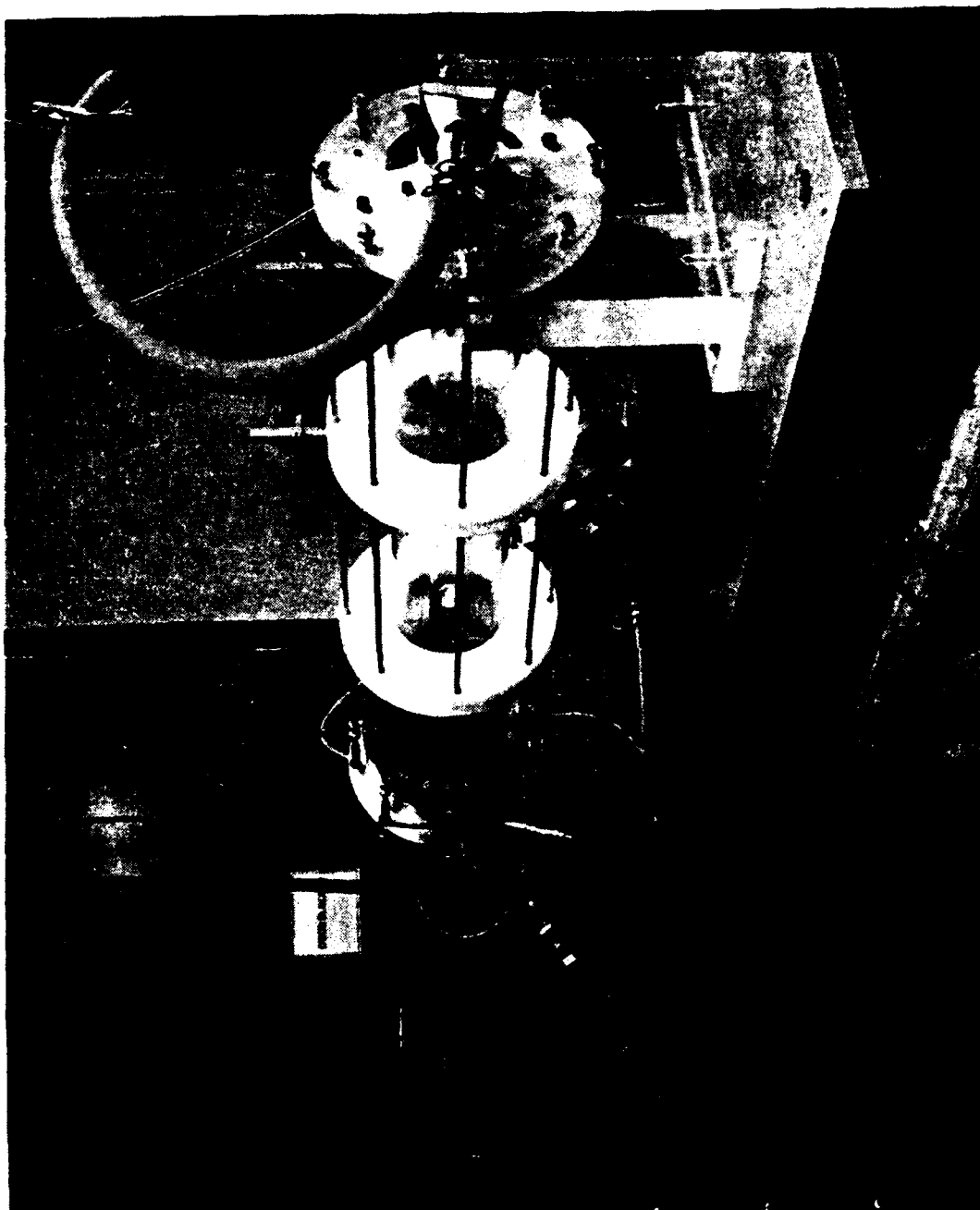


Figure 1. The iodine laser.

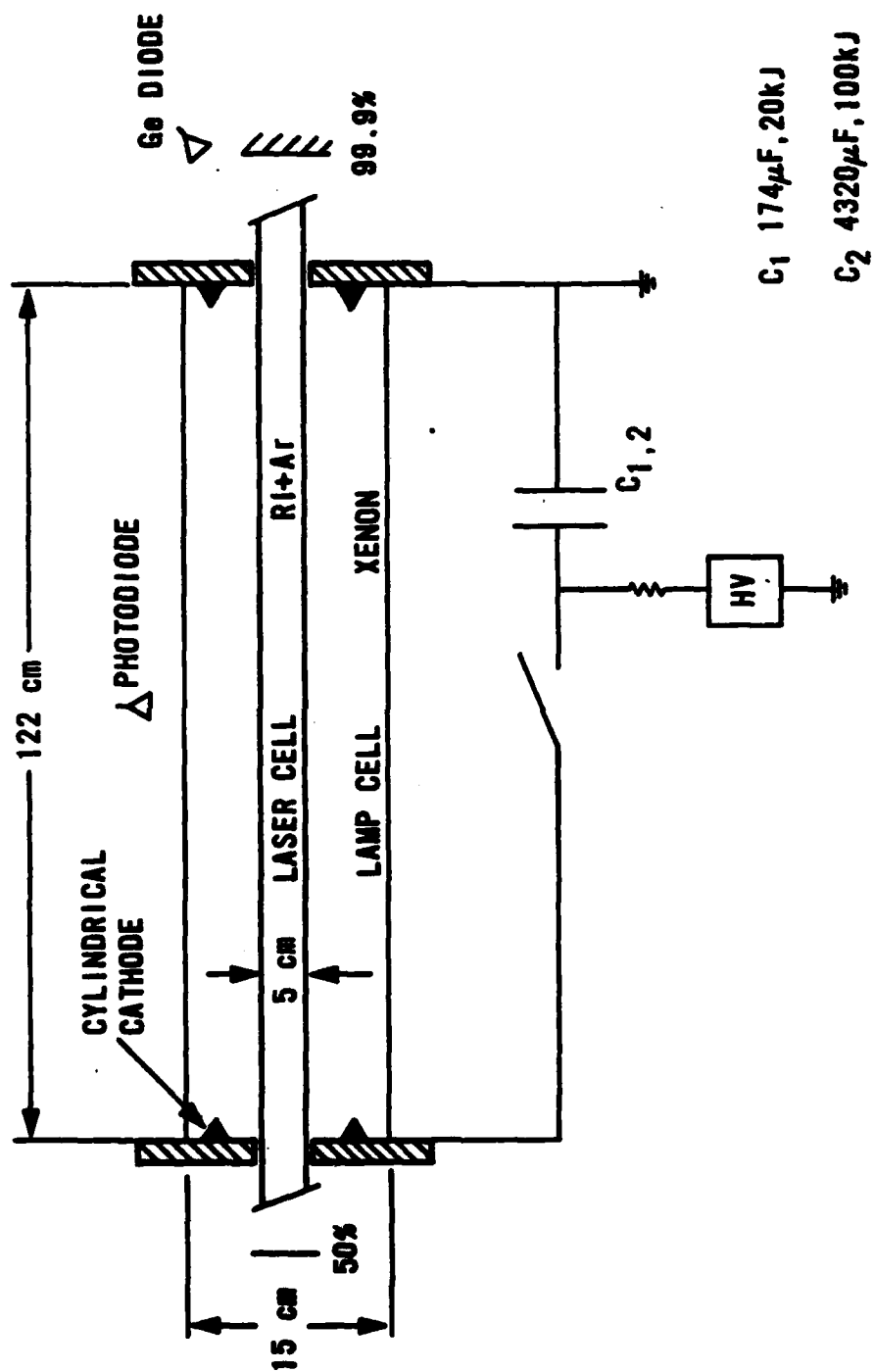
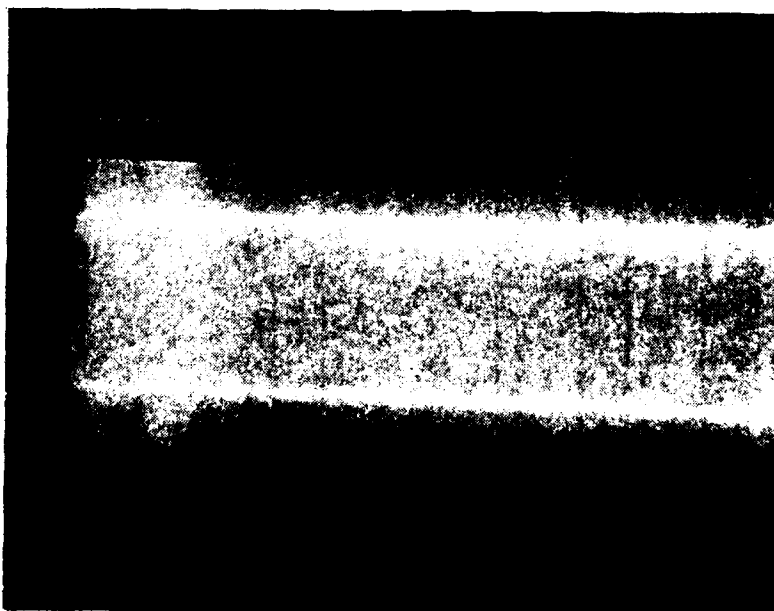


Figure 2. Laser schematic.



(a) Close-up view.



(b) Full-length view.

Figure 3. Open-shutter photos of the Z-pinch discharge.

The increased current density also excites additional xenon line radiation in the pump band of the CF_3I molecule. A further advantage of the geometry in Figure 2 is the close coupling of the pump radiation to the laser cavity.



Accession For	
NTIS GRA&I	<input checked="checked" type="checkbox"/>
DTIC TAB	<input type="checkbox"/>
Unannounced	<input type="checkbox"/>
Justification	
By	
Distribution/	
Availability Codes	
Dist	Avail and/or Special
A-1	

II. THE EXPERIMENT

In the first phase of the experiment, a 174- μ F capacitor bank was charged to typically 15 kV, yielding a maximum available bank energy of 20 kJ. The bank was triggered by four ignitrons connected in parallel. Current return was provided by the brass rods external to the laser shown in Figure 1. This coaxial return path inhibited magnetic nonuniformities which would destabilize the plasma pinch. Additional ignitrons were used as crowbars to prevent oscillation of the bank. In the second phase of the experiment, a 4320- μ F bank was charged to typically 6 kV, producing 77 kJ of available energy. Unless otherwise stated, all results discussed are with respect to the larger bank.

The resonator consisted of two flat 7.5-cm mirrors, coated for 99.9 percent and 50 percent reflectivity at 1.315 μ m. A Rogowski coil was used to monitor the discharge current. A voltage divider was connected between high voltage and ground to monitor the transient voltage. It consisted of ten 10-k Ω resistors in series with a 50- Ω current transformer. A visible photodiode monitored the lamp output and a germanium diode was placed opposite the angled quartz cavity windows to monitor the laser output. Laser energy was measured using a Scientech Model 540 calorimeter.

The time-resolved diagnostics can be interpreted via a simple model of the dynamic pinch. In the so-called "snow-plow" model (Ref. 4), we assume a zero rise time for the applied voltage, a perfectly conducting plasma, and a negligible plasma kinetic pressure inside the current shell during the compression. The current will then be constrained to flow in a thin shell with a solely external field, B_0 , producing inward radial acceleration.

The magnetic field outside the current shell is given by

$$B = \frac{\mu_0}{2\pi} \frac{I}{r} \quad (3)$$

4. Krall, N., and Trivelpiece, A., Principles of Plasma Physics, pp. 123-128, McGraw-Hill, 1973.

The total shell mass per unit length is

$$M = \rho_m(t=0)\pi(a^2 - R^2) \quad (4)$$

where R is the radius of the shell at time t , and a is the location at $t = 0$, which is 6.21 cm. The fluid velocity is

$$v = \frac{dR}{dt} \quad (5)$$

and from the momentum equation

$$\frac{d}{dt} \rho_m(R) \frac{dR}{dt} = \sqrt{4\pi\epsilon_0} J_Z B_\theta \quad (6)$$

The volume of the current shell is $2\pi R \Delta R$, so $\rho_m(R) = M/\text{vol}$ and $J_Z = I/(2\pi R \Delta R)$. The equation of motion for the shell becomes

$$\frac{d}{dt}(M) \frac{dR}{dt} = IB \quad (7)$$

We can transform to dimensionless variables to give the snow-plow model equation of motion, assuming a linear current rise

$$\frac{d}{d\tau} \left[(1-x^2) \frac{dx}{d\tau} \right] = -\frac{\tau^2}{x} \quad (8)$$

where

$$x = \frac{r}{a} = \frac{\text{radius}}{\text{initial radius}}$$

$$\tau = \frac{t}{t_1} = \frac{\text{time}}{\text{time scale for compression}}$$

$$t_1 = \left[\frac{ar}{(dI/dt)} \right]^{1/2} M_0^{1/4}$$

and

$$M_0 = \pi a^2 \rho_m = \text{total mass of gas per unit length of plasma at beginning of compression}$$

With initial conditions of $x(0) = 1$ and $(dx/d\tau)_0 = 0$, Equation 8 can be integrated numerically, with the result shown in Figure 4.

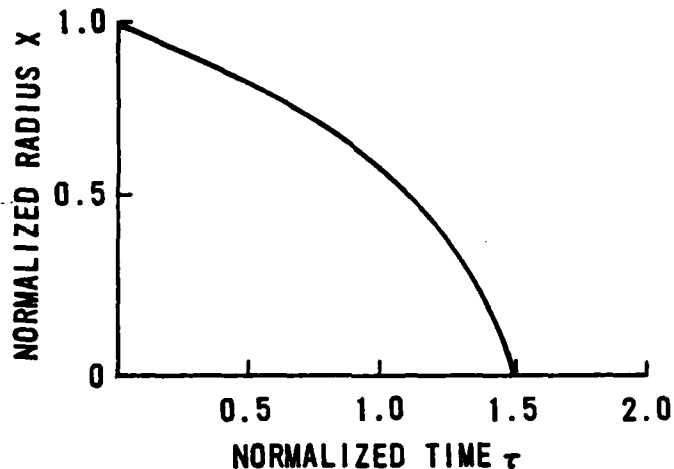


Figure 4. Z-pinch normalized radius versus time.

Representative experimental results are shown in Figure 5. The snow-plow model predicts a collapse time about half that of the experiment. The predicted collapse time is taken from Figure 4 by reading the normalized time, τ , at the point on the curve corresponding to the radius of the inner tube, since the pinch terminates at the inner tube radius of 2.86 cm. The longer experimental collapse time results from a nonlinear current rise, a finite plasma kinetic pressure, and any nonuniformities in the discharge.

A typical laser burn pattern is shown in Figure 6. The associated diagnostic monitor outputs are shown in Figure 7. The burn exhibits an interference pattern due to the slight wedge on the 50 percent output mirror. Since the mirror does not have an antireflection coating on the second surface, a standing wave is built up between the two surfaces and thus produces the interference. The gain of the laser is sufficiently high that lasing also occurs without the coated optics. Figure 8 shows two burn patterns, with and without resonator optics.

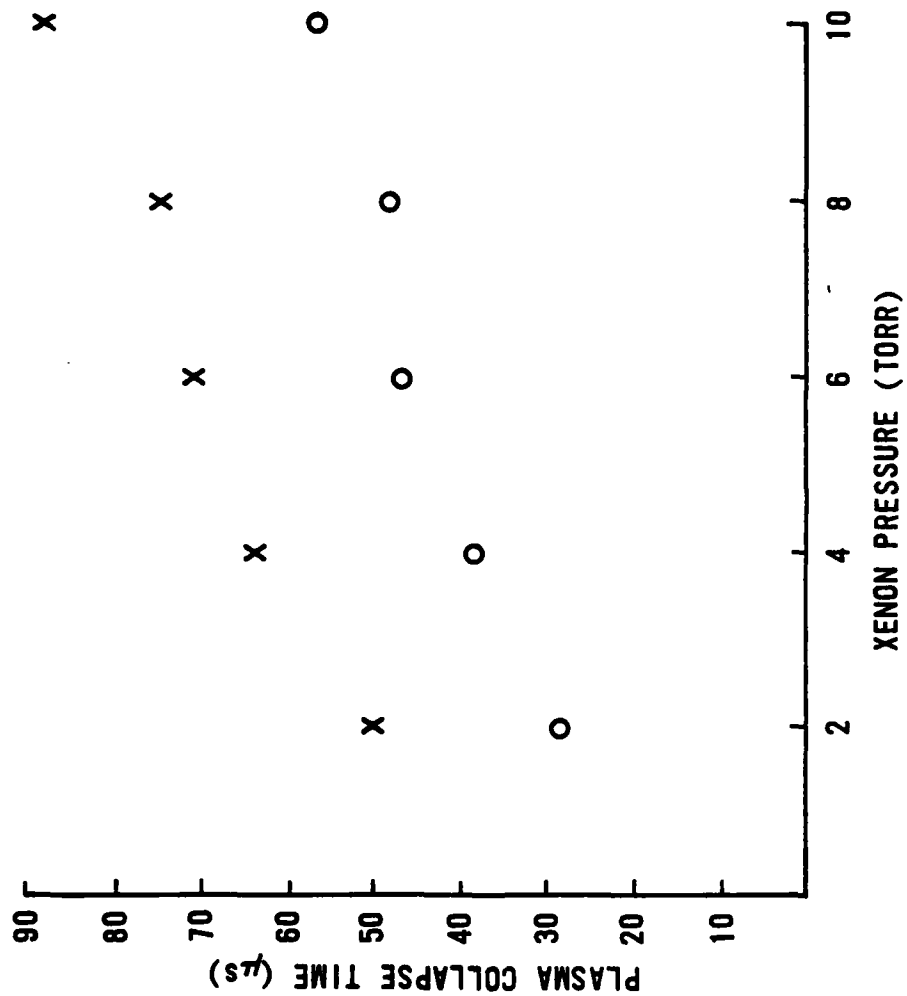


Figure 5. Experimental (x) and calculated (o) times for the plasma to collapse against the inner quartz tube.

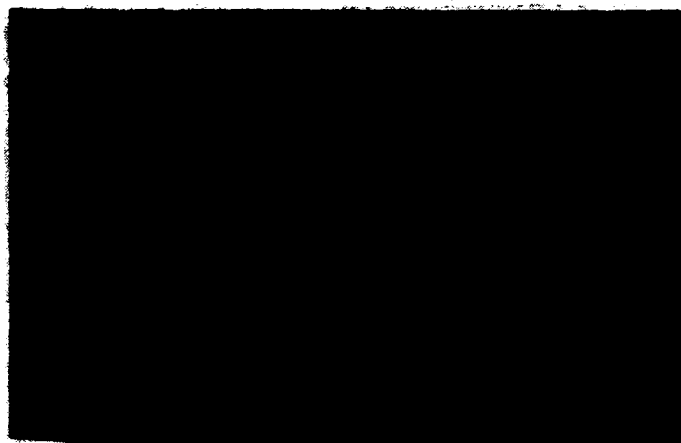


Figure 6. Laser burn pattern.

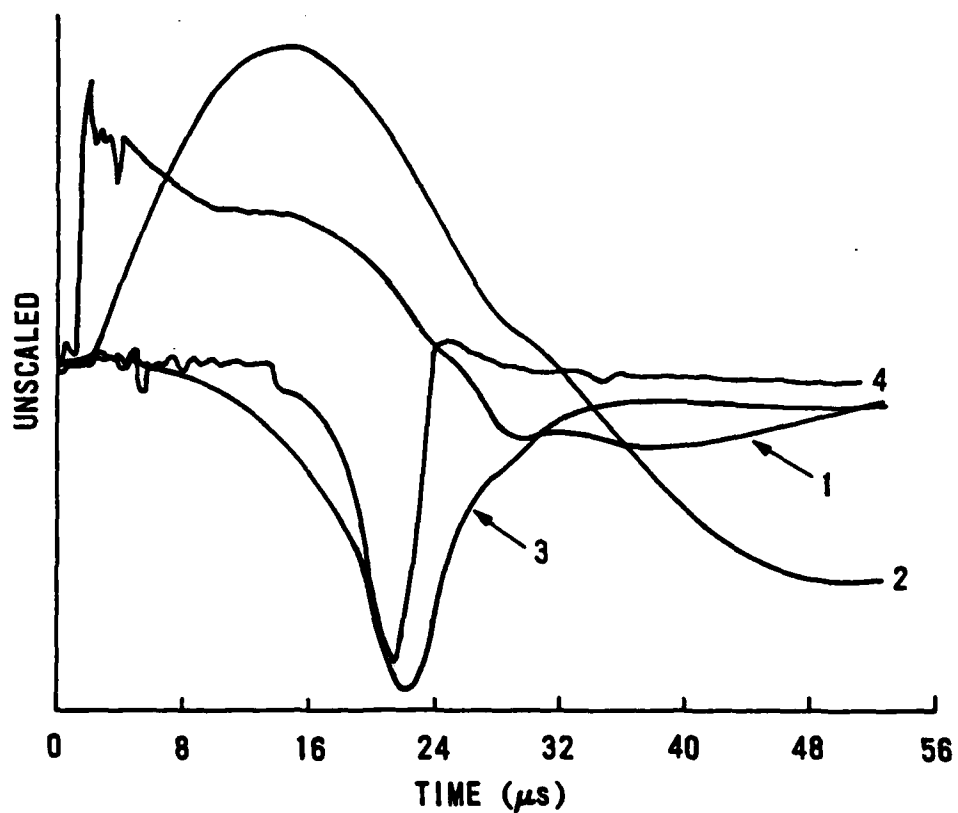
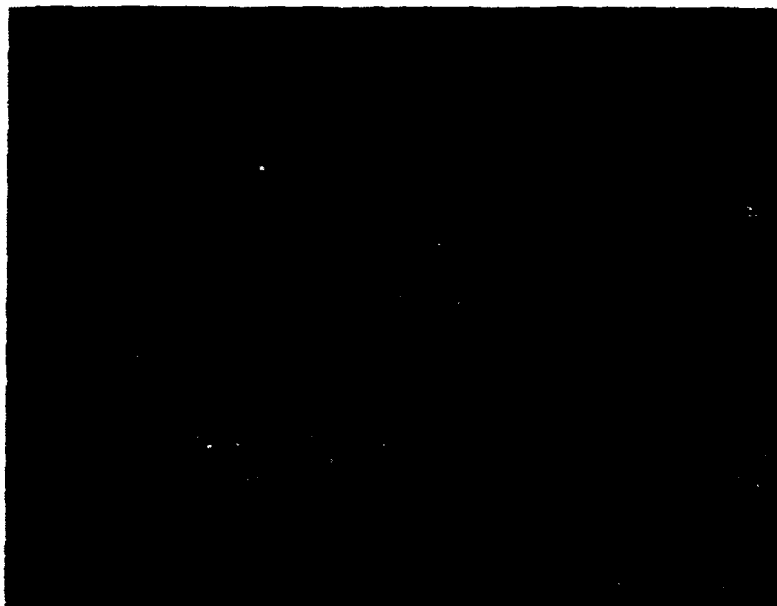


Figure 7. Diagnostic traces for the shot of Figure 6: Curve 1 - voltage
2 - current; 3 - visible light; 4 - laser pulse.



(b) Without resonator optics.



(a) With resonator optics.

Figure 8. Laser burn patterns.

The greatest laser energy achieved was 30.1 J at a bank voltage of 6 kV and a xenon pressure of 800 Pa. An interesting case was observed at a xenon pressure of 267 Pa. The measured laser energy was 28 J, delivered by two laser pulses separated by about 30 μ s. Figure 9 shows the diagnostic record. At this low xenon pressure, the plasma shell bounces off the inner tube, but there is enough electrical energy to compress it again. Figures 7 and 9 both show that the laser pulse follows the flash lamp output on the rising portion, but cuts off much more sharply on the falling portion. This is because the gain falls below threshold late in the pulse via chemical deactivation and ground state buildup.

A set of traces that shows the multiple pinch effect perhaps more clearly is shown in Figure 10. The double current dip and laser pulse are well pronounced along with the voltage rise from the increased impedance as the shell collapses each time.

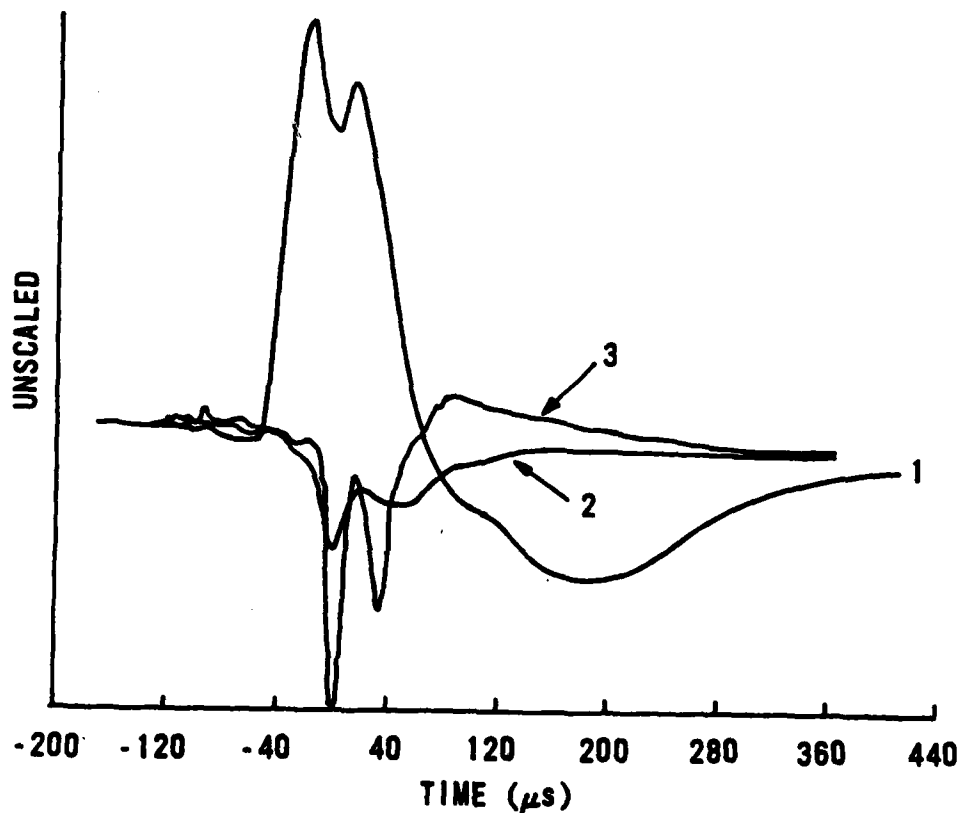


Figure 9. Diagnostic traces: Curve 1 - current; 2 - visible light; 3 - laser pulse.

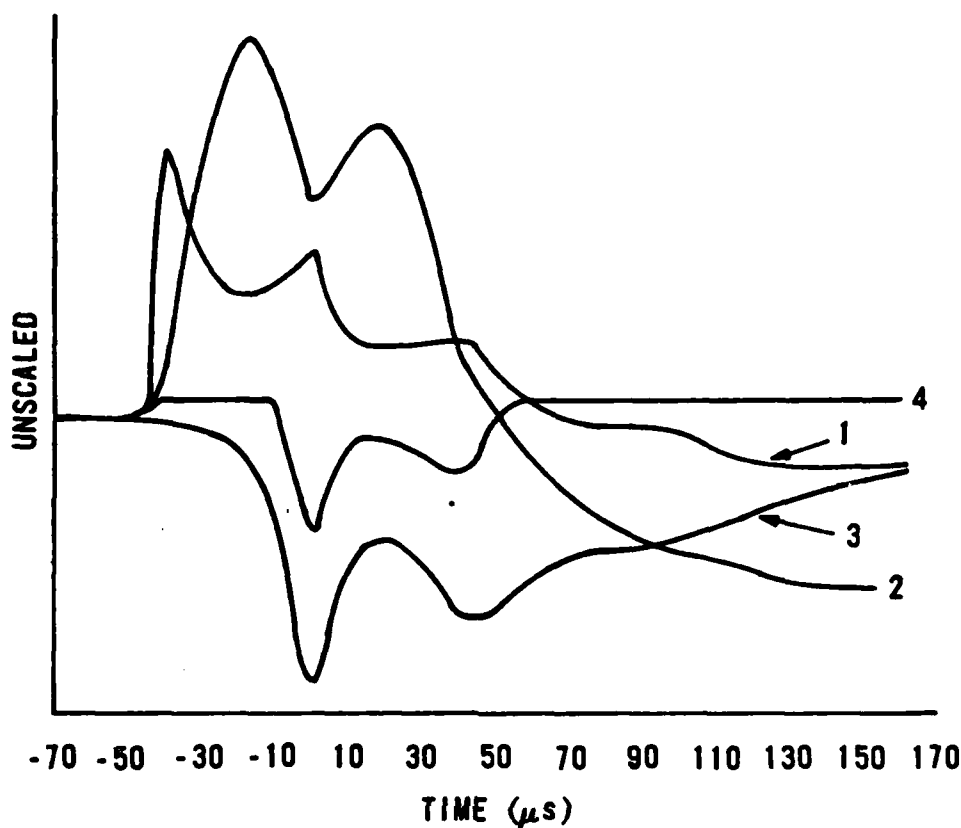


Figure 10. Diagnostic traces: Curve 1 - voltage; 2 - current; 3 - visible light; 4 - laser pulse.

Figure 11 shows the results from varying xenon pressure from shot to shot at a bank voltage of 6 kV and CF_3I pressure of 13,332 Pa. The flash lamp output pulse length increases with xenon pressure. The laser output energy is relatively constant, except for a dip around 1200 Pa to 5 J. This pressure is too high to dynamically pinch and is too low for very successful resistive heating of the xenon plasma. Therefore, the initiation is diminished along with the laser energy.

Increasing the CF_3I pressure above 6666 Pa resulted in absorption of the bulk of pump radiation in an annulus, as shown by the laser burn pattern results of Figure 12. The UV absorption cross section for the CF_3I molecule is shown as a function of wavelength in Figure 13. An approximate average value for the penetration depth is given by $\lambda = 1/\alpha \approx (1.33 \times 10^4 \text{ Pa-cm})$. From Figure 12, it

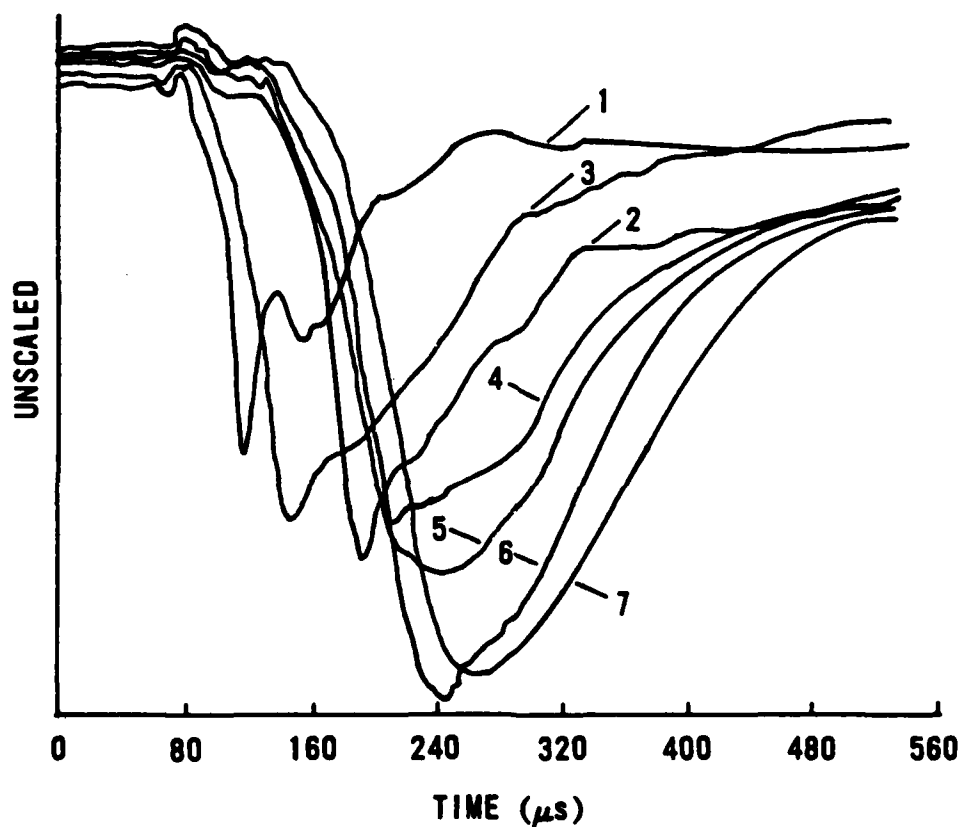
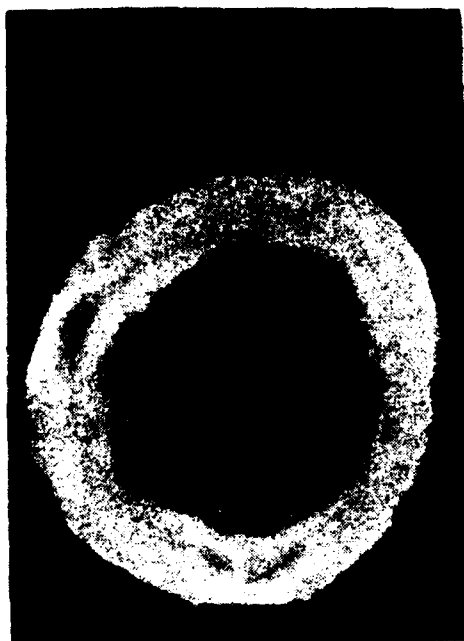
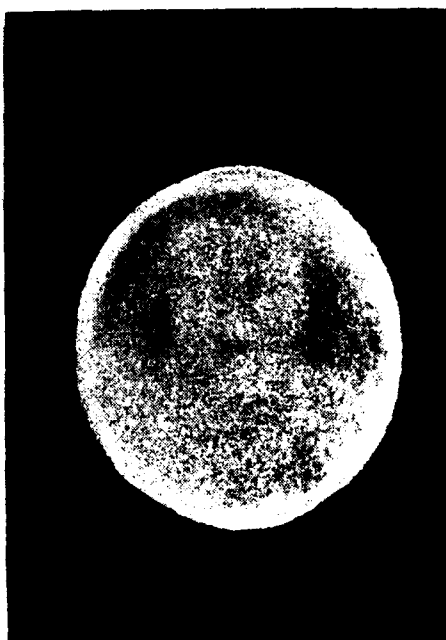


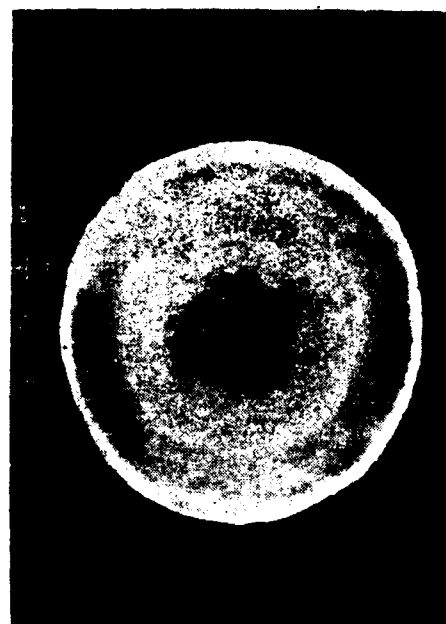
Figure 11. Visible light traces for various xenon pressures:
 Curve 1 - 267 Pa, laser energy 22.9 J; Curve 2 - 800 Pa, laser energy 22.3 J; Curve 3 - 1067 Pa, laser energy 25.2 J; Curve 4 - 1333 Pa, laser energy 16.3 J; Curve 5 - 2000 Pa, laser energy 22.3 J; Curve 6 - 4000 Pa, laser energy 23.2 J; Curve 7 - 6666 Pa, laser energy 18.6 J.



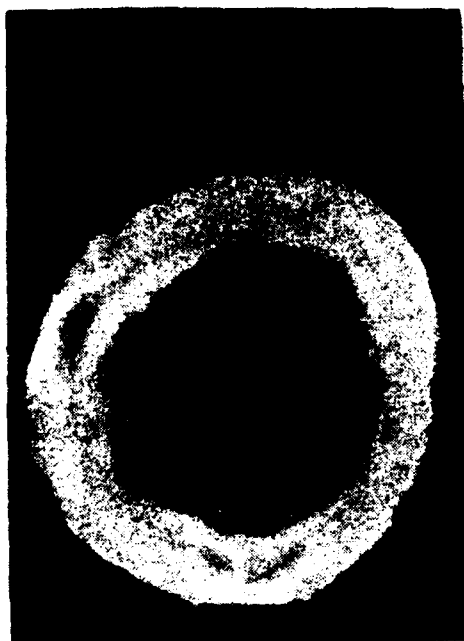
(a) 2×10^4 Pa.



(c) 9.33×10^3 Pa.



(d) 6.67×10^3 Pa.



(b) 1.33×10^4 Pa.

Figure 12. Laser burn patterns for various CF_3I pressures.

is seen that laser power sufficient to burn Polaroid film occurs in an annulus slightly thicker than λ . The weak burning inside the annulus must be due to UV radiation on the wings of the curve in Figure 13. Laser power can be increased by increasing the amount of pump radiation or by shifting more pump energy to the wings of the absorption curve.

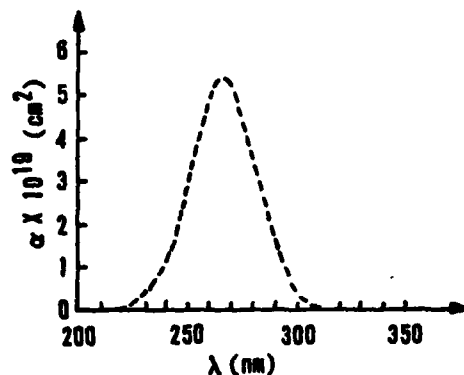


Figure 13. CF_3I absorption band (Ref. 2).

The half-angle divergence of the laser was approximately 2 mrad. This was measured by comparison of burn patterns at short range (Fig. 8) with burn patterns at 6 m (Fig. 14).



Figure 14. Laser burn pattern at 6 m.

The damage threshold of the resonator optics was determined qualitatively. A 2.5-cm sample substrate was coated for maximum reflectivity at 1315 nm. Laser pulses were focused by lenses onto the sample at increasing levels of fluence. The focused beam was not very uniform, as shown by the burn pattern in Figure 15. The existence of hot spots implies that the damage threshold measured for an average fluence level is a minimum value. At 5 J/cm^2 , no damage was visually observed. At 7 J/cm^2 , small pit marks were seen randomly across the exposed coating area. At 10 J/cm^2 , the coating was severely damaged throughout the exposed area. The measurements were taken prior to a decision whether to purchase coated or metal optics for a follow-on scaled-up iodine laser. For a high-energy device, i.e., with fluences greater than 5 J/cm^2 , metal optics are the preferred choice.



Figure 15. Focused laser burn pattern.

A spectroscopic study was made of the radiation emitted in the pump band by the flash lamp. A conical aluminum reflector was placed in the center of the quartz laser tube, directing pump light axially toward a 0.25-m monochromator (Fig. 16). A calibrated deuterium source provided standard intensities as a function of wavelength (Fig. 17). The transmission spectral response of the quartz tube was scanned through the pump band and found to be effectively unity. The conical reflector was shown to be a point source of flash lamp radiation by plotting PMT peak output voltage versus $1/R^2$, where R is the distance from the reflector to the monochromator (Fig. 18).

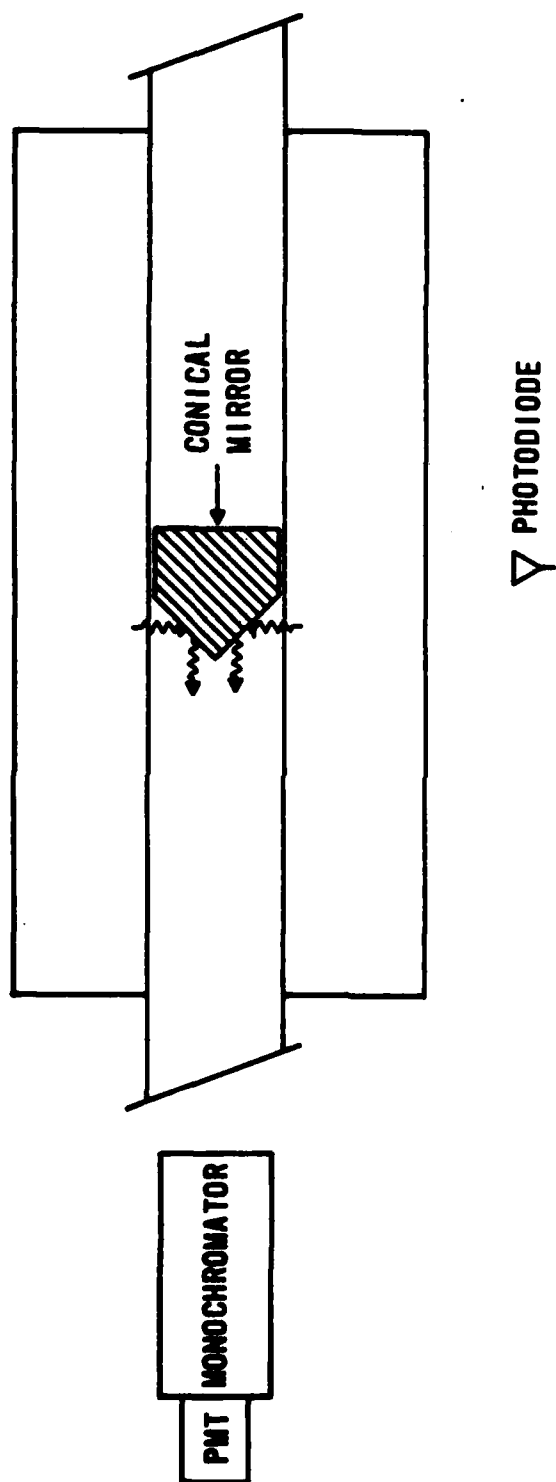


Figure 16. Spectral measurements schematic.

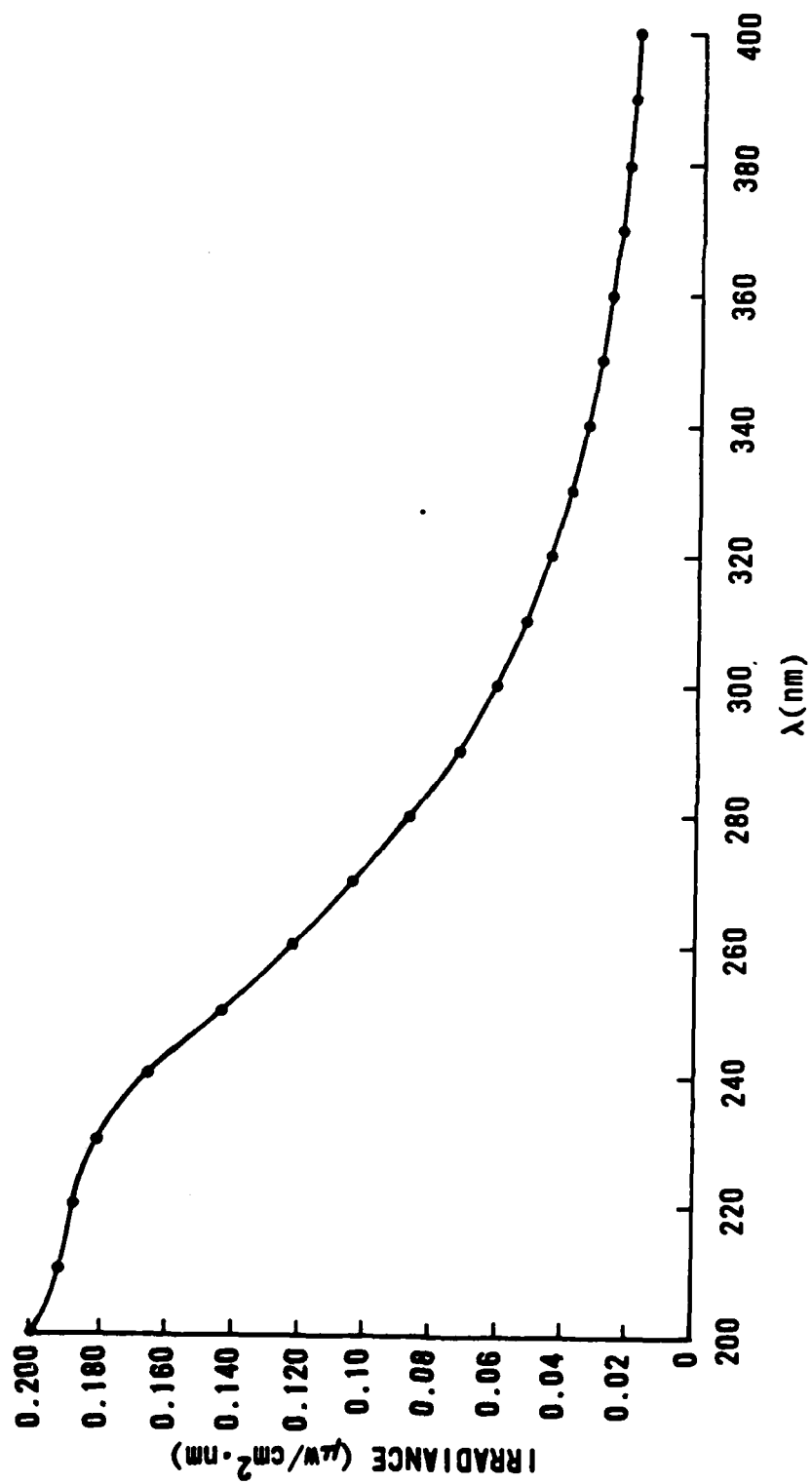


Figure 17. Calibrated D₂ lamp output.

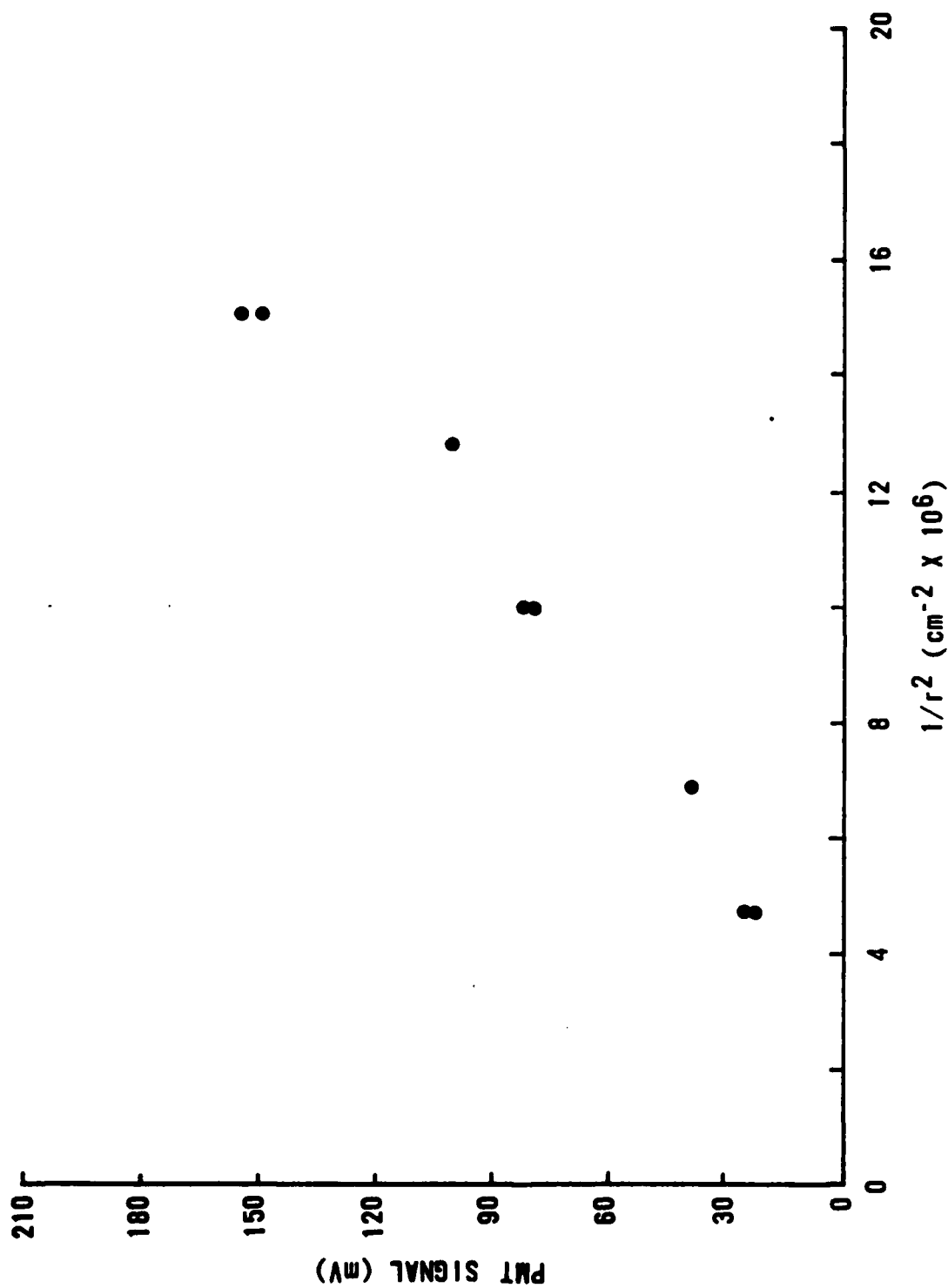


Figure 18. Flash lamp radiation peak intensity versus inverse squared distance from the monochromator.

A scan of pump band light from 267-6666 Pa xenon was made at a monochromator setting of 270 nm and an entrance slit opening of 0.3 mm. The results are shown in Figure 19.

A scan of pump band radiation from 230 nm to 300 nm was performed in 5-nm increments by opening the monochromator slits wide enough to pass a 5-nm band centered at each recorded wavelength. The reflectivity of the cone and the monochromator optics varies with wavelength and was taken into account in the final results. Figure 20 shows the reflectivity of three points on the polished flat rear of the cone, exhibiting both spatial and wavelength variations. The wavelength dependence of the monochromator optics is shown by a scan of the D₂ source (Fig. 21). A comparison of Figures 17 and 21 reveals the monochromator optics response falloff at short wavelengths.

Folding in the wavelength dependent calibration factors, the normalized results are shown in Figure 22, represented by the peak intensity values. The two scans done at 800 Pa Xe were done sequentially to determine repeatability, which was quite good. The scan at 4000 Pa Xe reveals higher integrated energy, but less peak power. This is demonstrated by comparing Figures 23 and 24 which show the diagnostic traces for the 800-Pa and 4000-Pa cases at a particular wavelength, 255 nm, along with the respective integrated energies.

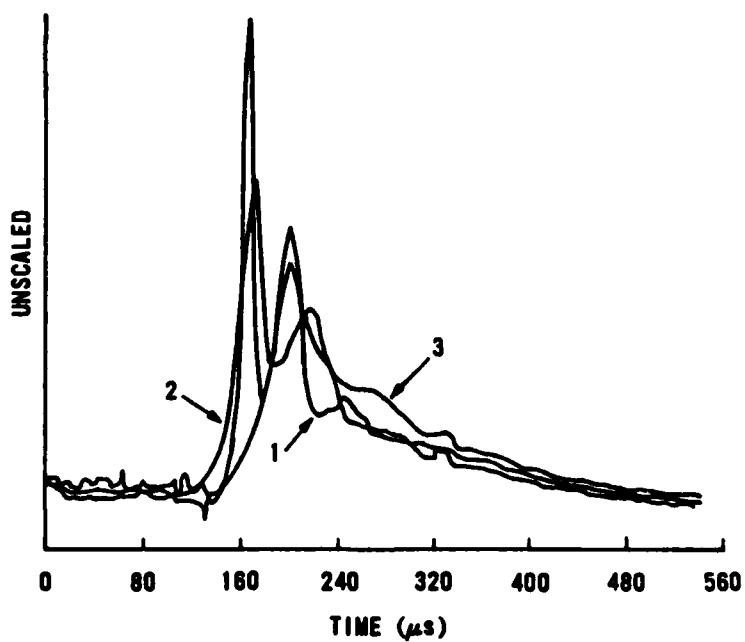
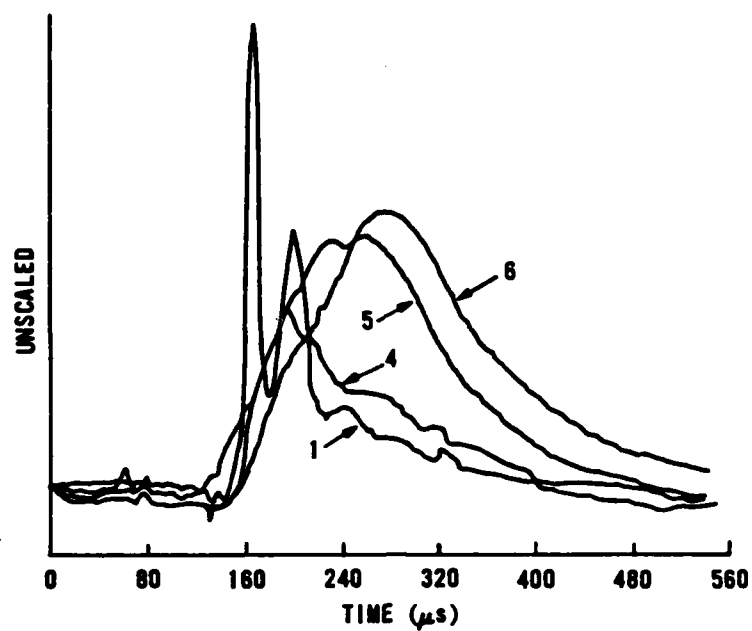


Figure 19. Pump band flash lamp radiation for various xenon pressures:
 Curve 1 - 267 Pa; Curve 2 - 800 Pa; Curve 3 - 1333 Pa;
 Curve 4 - 2000 Pa; Curve 5 - 4000 Pa; Curve 6 - 6666 Pa.

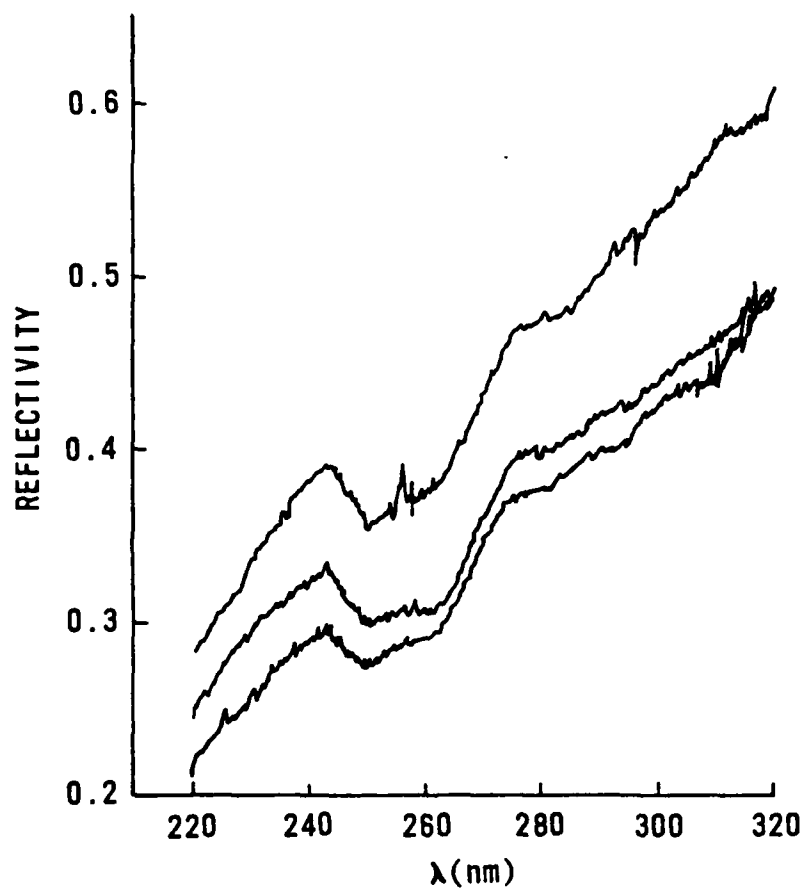


Figure 20. Reflectivity versus wavelength for three points on the conical reflector.

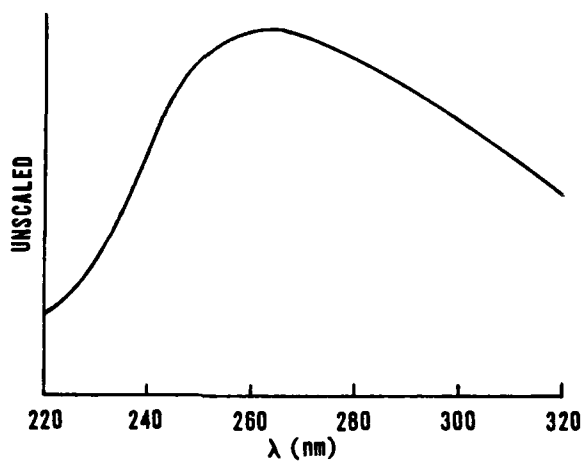


Figure 21. D₂ lamp intensity versus wavelength as measured through the monochromator.

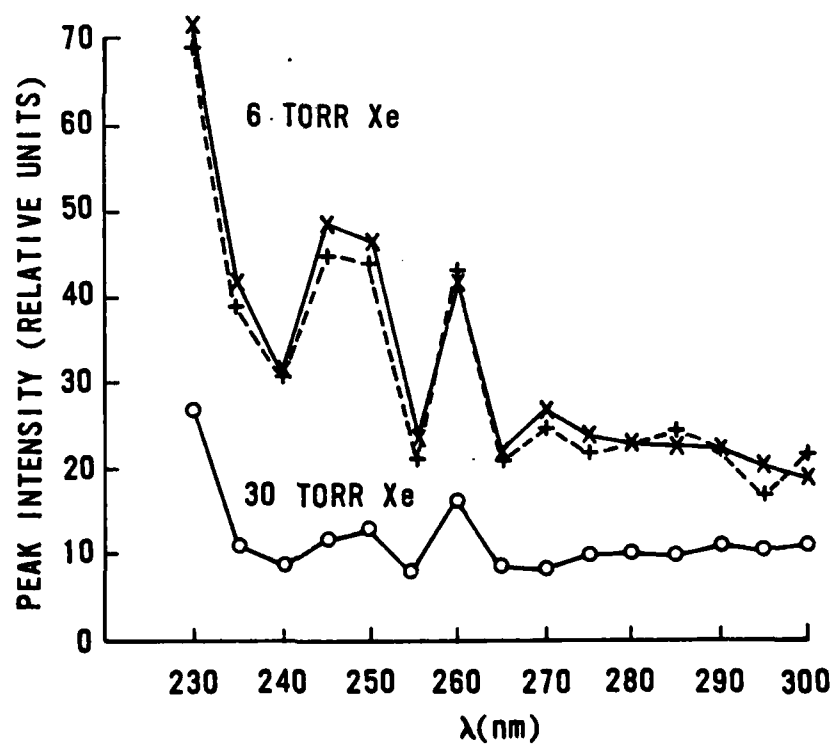


Figure 22. Flash lamp intensity versus wavelength.

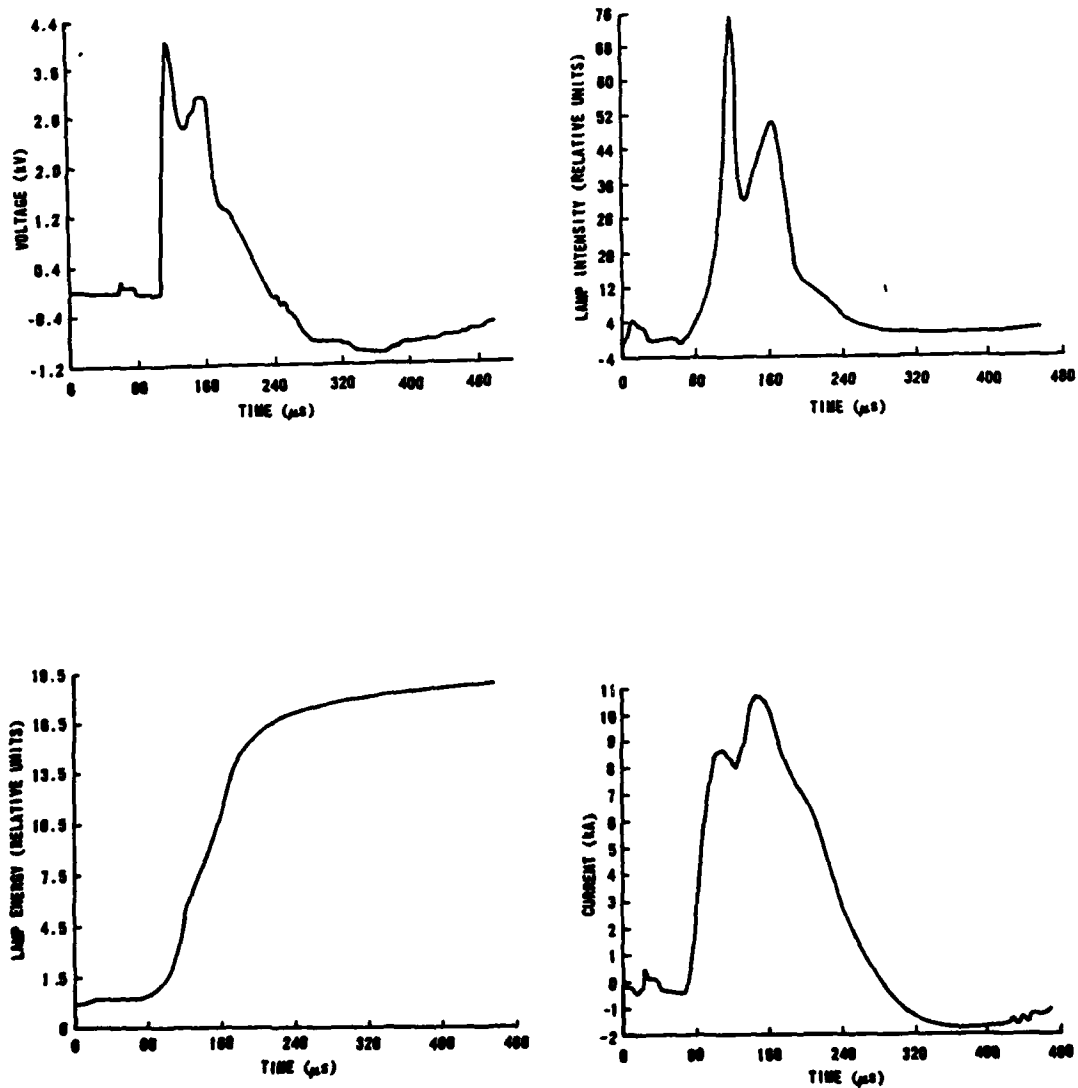


Figure 23. Diagnostic traces at 800 Pa xenon.

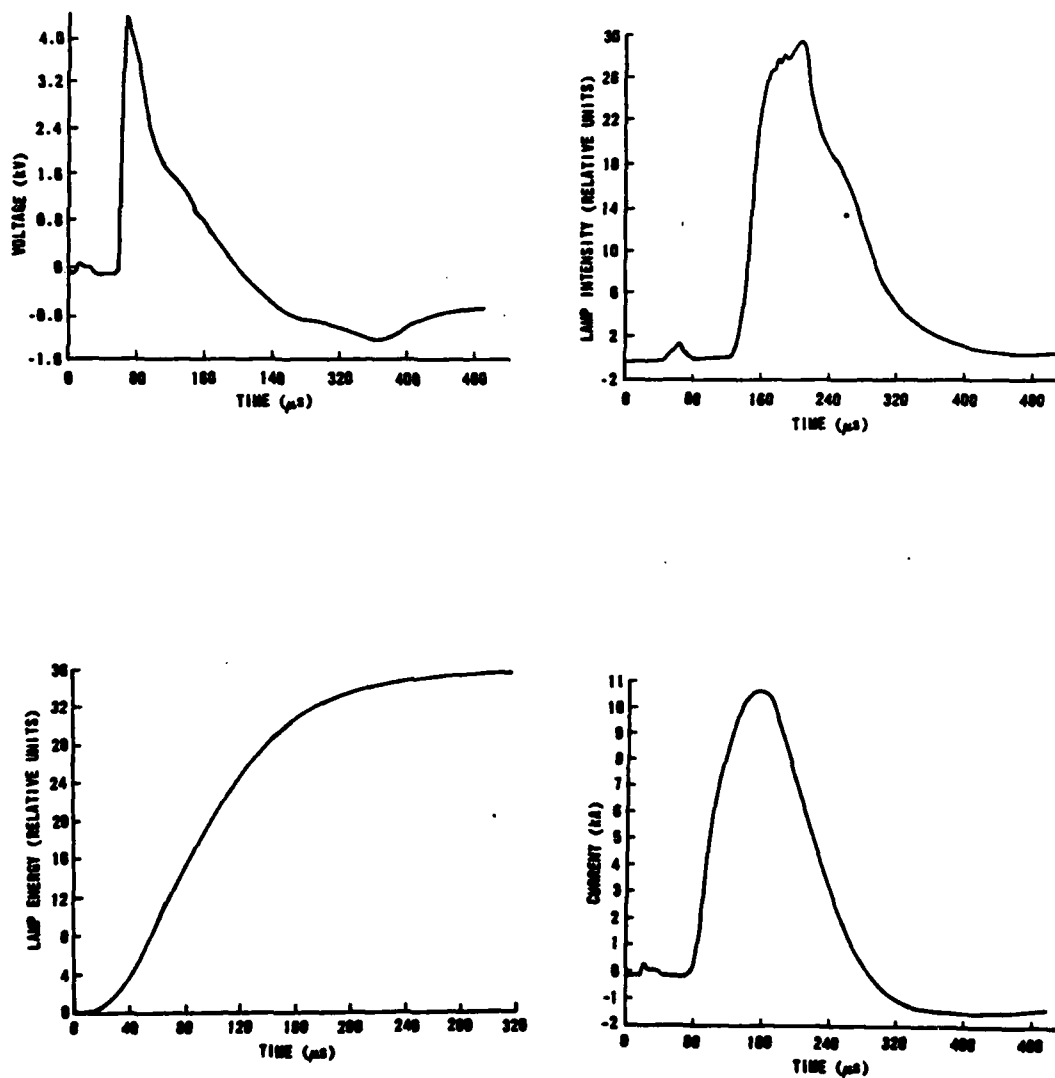


Figure 24. Diagnostic traces at 4000 Pa xenon.

III. CONCLUSIONS AND RECOMMENDATIONS

The Z-pinch flash-initiated iodine laser is a workable device under quite varied conditions. With high-pressure windows to allow increased CF_3I and diluent concentrations, laser energy could be easily increased with the existing electrical setup. Scaled-up versions of the laser could employ either low- or high-pressure xenon flash lamps, depending on the desired pulse length.

A scaled-up version using existing copper resonator optics, quartz tubes, and capacitors could be used to produce gas channel density gradients via laser absorption. This would allow studies of electron beam propagation in dynamically rarefied channels, although the gas would necessarily be some organic molecule absorptive at $1.315 \mu\text{m}$. Air is transmissive at that wavelength. Q-switching could also be employed to generate high peak powers in order to produce conductivity channels for electron beam experiments.

END

DATE
FILMED

5 - 84

DTIC

